

Near-threshold collisional dynamics in the e^-e^+p system

H. B. Ambalampitiya^{1,2}, J. Stallbaumer,² I. I. Fabrikant², I. Kalinkin,³ D. V. Fursa³, A. S. Kadyrov^{3,4} and I. Bray³

¹*Quantemol Ltd., 320 City Road, London EC1V 2NZ, United Kingdom*

²*Department of Physics and Astronomy, University of Nebraska–Lincoln, Lincoln, Nebraska 68588-0299, USA*

³*Department of Physics and Astronomy, Curtin University, GPO Box U1987, Perth, Western Australia 6845, Australia*

⁴*Institute of Nuclear Physics, 100214 Ulugbek, Tashkent, Uzbekistan*



(Received 22 March 2023; accepted 18 August 2023; published 8 September 2023)

We study $e^+H(n)$ and $Ps(n)-p$ collisions near the three-body breakup threshold and thresholds for the charge-transfer processes. We show that classical trajectory Monte Carlo (CTMC) simulations for the three-body breakup agree reasonably well in this energy region with quantum-mechanical convergent close-coupling (CCC) calculations even if the initial hydrogen atom or positronium atom is in the ground state. The threshold behavior of the three-body breakup cross section in $e^+H(1s)$ and $Ps(1s)-p$ collisions agrees with the Wannier law with Klar's exponent and obeys the classical scaling laws, although some deviation from the Klar-Wannier behavior is observed in the CCC results. Below the threshold the agreement between CTMC and CCC disappears. In particular the CTMC method fails completely for the processes of H formation in $Ps(1s)-p$ collisions and Ps formation in e^+H collisions well below the three-body breakup threshold. For higher initial states the CTMC results below the threshold improve substantially, in accordance with the correspondence principle. This is explained by comparing the quantum-mechanical threshold laws with the classical laws.

DOI: [10.1103/PhysRevA.108.032808](https://doi.org/10.1103/PhysRevA.108.032808)

I. INTRODUCTION

The threshold laws are ubiquitous in collision processes [1]. It is important to understand the role of quantum effects in these laws. In particular, the Wigner threshold law [2] is purely quantum mechanical. For an endothermic reaction it appears as a manifestation of quantum suppression [3]. In contrast, the Wannier law [4] for electron-impact ionization of atoms was derived within the framework of classical mechanics and confirmed by the quasiclassical theory [5,6]. Although there is no formal proof of this law within the framework of the quantum-mechanical three-body problem, there is strong evidence that the three-body physics of particles interacting via the Coulomb force, near the threshold of the three-body breakup, is described adequately by classical mechanics. This is not surprising since low-energy Coulomb scattering is essentially classical [4,7]. However, until recently, the absence of accurate quantum calculations in the challenging near-threshold region prevented rigorous tests of Wannier physics. Recent convergent close-coupling (CCC) calculations of e^+H and $Ps-p$ collisions [8–12] have attempted to overcome this obstacle and allow detailed verification of the classical approach. On the other hand, with the increasing degree of excitation of reactants, quantum calculations become very challenging computationally, whereas classical calculations can be extended for higher states with the same computational efficiency. Moreover, due to the classical scaling laws the volume of the classical trajectory Monte Carlo (CTMC) calculations can be substantially reduced by rescaling results obtained for the ground target state. Note, however, that if the cross section is small, the number of trajectories in the CTMC method should be substantially increased in order to keep the relative error small. It is important therefore to investigate the validity of the classical methods in the near-threshold regions.

In the present paper we investigate the threshold behavior of several processes involving three particles interacting via Coulomb's law,

$$Ps(n) + p \rightarrow e^- + e^+ + p, \quad (1)$$

$$Ps(n) + p \rightarrow e^+ + H(n'), \quad (2)$$

$$e^+ + H(n) \rightarrow e^+ + e^- + p, \quad (3)$$

$$e^+ + H(n) \rightarrow Ps(n') + p, \quad (4)$$

where n is the principal quantum number, by using the CTMC method [13] and comparing the results with quantum CCC calculations. A more detailed investigation involving an analysis of initial and final angular momentum states of H and Ps is also possible [11,12], but the major physics is captured by looking at the n dependence. Therefore, we will be considering cross sections averaged over initial and summed over final angular momentum states. As a rule, we will also sum the cross sections over the final discrete n' states. Note that the charge-conjugated reactions, which have the same cross sections, are important for the antihydrogen formation, and they were studied in this context [10,11]. Here we will be discussing reactions involving p and H, but the same conclusions will be applicable to the charge-conjugated reactions involving \bar{p} and \bar{H} .

Reactions (3) and (4) near the three-body breakup threshold were studied using the CTMC method in [14,15] and, more recently, in [16]. Klar [17] obtained an extension of the Wannier law with e^- , e^+ , and p in the final state, which includes reactions (1) and (3). The cross section for these

reactions behaves as

$$\sigma = C(\Delta E)^\mu, \quad (5)$$

where C is a constant, ΔE is the energy relative to the threshold, and $\mu = 2.65$. This result was confirmed by semiclassical theories [18,19]. Moreover, Ihra *et al.* [19] and Jansen *et al.* [20], using the hyperspherical hidden-crossing theory, obtained an exponential correction to Eq. (5) which slows down the growth of the ionization cross section well above the threshold. Quantum CCC calculations [21] confirm the Klar prediction and the correction obtained in [19]. Measurements of positron-impact ionization of hydrogen [22] do not go close enough to the threshold to verify the Klar-Wannier law. Experimental data on the positron-impact ionization of He [23] confirm the Klar-Wannier law with the exponent close to that predicted by Klar, although more recent measurements with the argon atom [24] produced a much lower exponent, $\mu = 1.05 \pm 0.14$. The authors [24] suggested that their measurements, performed above $\Delta E = 0.2$ eV, were not close enough to the threshold to reproduce the Klar-Wannier law for Ar. However, for atomic hydrogen, as will be shown below, the range of validity of the Klar-Wannier law extends up to $\Delta E = 10$ eV.

The threshold behavior of reactions (2) and (4) depends on their threshold energies and the initial principal quantum number n . Reaction (2) (summed over all final states) is always exothermic and, for $n = 1$, obeys the Bethe-Wigner threshold law [2,25]

$$\sigma \propto E^{-1/2}, \quad (6)$$

where E is the incident center-of-mass energy. However, for $n > 1$ the hydrogen atom, due to the degeneracy of its excited states, possesses an effective dipole moment which makes the cross section for H formation diverge as E^{-1} [26,27], i.e.,

$$\sigma \propto E^{-1}. \quad (7)$$

In addition, partial cross sections exhibit Gailitis-Damburg oscillations [26,28] as a function of $\ln E$. However, these oscillations are not detectable in total cross sections, summed over the angular momentum for the relative motion [28]. The dipole threshold law is valid as long as we neglect the relativistic splitting between the excited states. Within the energy region where this splitting cannot be ignored the Bethe-Wigner law is restored. In the present paper we consider energies which are well beyond this region; therefore, we neglect the relativistic splitting.

The Ps formation reaction (4) is endothermic for $n = 1$; therefore, it obeys the Wigner law [2]

$$\sigma \propto (E - E_t)^{1/2}, \quad (8)$$

where $E_t = 0.25$ a.u. is the threshold energy. For $n > 1$ it becomes exothermic and obeys the dipole threshold law for an exothermic reaction, Eq. (7). Note that for partial $n \rightarrow n'$ cases the reaction can be endothermic if $n' > n\sqrt{2}$ for reaction (2) and if $n' > n/\sqrt{2}$ for reaction (4). In this case the quantum cross section, similar to the classical cross section, becomes finite at the threshold [26] if $n' > 1$. However, the threshold law, both its classical and quantum versions, does not say anything about the threshold value of the cross section which depends on the interaction in the reaction zone; therefore, the

threshold value of the cross section can be substantially different in classical and quantum theories. Similarly, the coefficient of proportionality in the threshold law for the exothermic case, Eq. (7), as well as the range of validity of the threshold law, can be substantially different in classical and quantum theories.

Our goal is to perform detailed studies of classical and quantum threshold behavior for reactions (1)–(4) for the ground and first few excited states. For highly excited states, as shown by previous studies [11,12,29–31], quantum and classical cross sections converge quickly, according to the generalized correspondence principle [32]. Although the principle was originally applied to ion-atom collisions, it works rather well even for collisions involving excited-state Ps. The reason for this is that Ps in excited states interacts with the proton by effectively dipolar force, and the scattering laws involving dipolar interactions are similar in quantum and classical mechanics [31].

Atomic units are used throughout unless stated otherwise.

II. THE CTMC METHOD

The CTMC theory for a three-body system consisting of charged particles in which two of them are bound was described in Refs. [13,33]. The CTMC approach was applied before in the case of a Ps atom interacting with a proton with no external field [11,29–31] and was recently extended to the laser-assisted case [34]. The theory is described in brief as follows. For a given impact parameter and the principal quantum number n_{Ps} of the projectile Ps atom, an ensemble of initial states is prepared by a random selection of the eccentricity, the orientation of the mutual motion (Kepler orbits) of the e^-e^+ pair, and the position of e^- on the orbit. A classical trajectory for each random state is then propagated towards the proton which is stationary at the origin of the configurations space. A similar procedure is performed for e^+ -H collisions.

The Hamilton equations of motion are solved using the regularization method described in [35,36]. The solutions are propagated, giving sufficient time for the interaction of the projectile (Ps or e^+) with the target (p or H). At the end of the propagation, the final energies and the angular momenta of the trajectories are checked to generate the statistics in different final channels to calculate the probabilities and cross sections. For example, the charge-transfer probability $P(b)$ as a function of the impact parameter b is computed as a ratio between the number of trajectories leading to the formation of the final atom and the total number of sampled trajectories. The charge-transfer cross section σ_{CT} is then given by the integral $\int 2\pi P(b) b db$. The total number of trajectories for each energy point was varied between 6×10^4 and 10^6 to make sure that the typical statistical error for the cross section is less than 2%. However, when the cross section is small, particularly for ionization near the threshold, the error can significantly exceed this limit, sometimes reaching 30%.

In the process of our calculations we have found that the charge-transfer cross section exhibits regular oscillations with small amplitudes which are beyond the statistical uncertainty of the CTMC method. We found out that these are an artifact of classical calculations which start with a fixed position of the

projectile in the configuration space. These oscillations and the process of their elimination are discussed in the Appendix.

III. CONVERGENT CLOSE-COUPPLING METHOD

The two-center convergent close-coupling method for positron-hydrogen scattering was developed by Kadyrov and Bray [8]. It explicitly incorporates Ps formation with convergence in terms of the basis size, which has to be checked for both the H and Ps centers. As a truncated complete Laguerre basis is used for both centers, the two nonorthogonal expansions lead to a highly ill-conditioned system of linear equations. This manifests as numerical problems when large expansions are used, for example, near-threshold regions in Charlton *et al.* [12]. Generally, the smaller the required cross sections are, the larger the expansions must be to obtain convergence. However, if the larger expansions lead to particularly ill-conditioned linear equations, then obtaining accurate results for the smaller cross sections can become problematic. In part, the motivation for the present CCC calculations is to obtain, as accurately as possible, near-threshold cross sections for the excitation of states with principal quantum number $n \leq 3$.

The CCC calculations are parametrized by the Laguerre basis orbital angular momentum quantum number $l \leq l_{\max}$, basis size N_l , and exponential falloff λ_l . In the case of two-center calculations these are independent for the two centers. For simplicity, we take $N_l = N_0 - l$ and $\lambda_l = \lambda$. The CCC calculations of Charlton *et al.* [12] had $l_{\max} = 9$ and $N_0 = 30$ for both centers, with $2\lambda_{\text{Ps}} = \lambda_{\text{H}} = 0.5$. Here we take $l_{\max} = 4$ and $N_0 = 25$ for both centers, with $2\lambda_{\text{Ps}} = \lambda_{\text{H}} = 1$.

The two-center CCC calculations of the underlying matrix elements rely on analytical expansions for their sufficiently rapid computational evaluation, which has been implemented only for $N_0 \leq 30$. Owing to potential precision loss associated with such expansions, here we utilize calculations with $N_0 = 25$. This limitation is unfortunate as in the near-threshold region for breakup we require large basis sizes in order to have sufficiently many open positive-energy pseudostates which represent the breakup. This shall be discussed further below when considering the corresponding breakup by electrons.

IV. CLASSICAL SCALING LAWS

The classical motion in a system of charged particles is invariant under the following scaling rules [13,37,38]:

$$\mathbf{r}' = \alpha^2 \mathbf{r}, \quad t' = \alpha^3 t. \quad (9)$$

Consider a collision characterized by the center-of-mass energy E and impact parameter b involving a hydrogenlike system (target) with initial energy ϵ and angular momentum L . Then the following scaling law for the collision probability can be obtained from (9):

$$P_{\epsilon L}(E, b) = P_{\epsilon/\alpha^2, \alpha L}(E/\alpha^2, \alpha^2 b). \quad (10)$$

For the cross section integrated over the impact parameter we obtain

$$\sigma_{\epsilon L}(E) = \alpha^{-4} \sigma_{\epsilon/\alpha^2, \alpha L}(E/\alpha^2). \quad (11)$$

Choosing $\alpha = 1/n$, where n is the principal quantum number of the target, we have

$$P_{nL}(E, b) = P_{1,L/n}(n^2 E, b/n^2) \quad (12)$$

and

$$\sigma_{nL}(E) = n^4 \sigma_{1,L/n}(n^2 E). \quad (13)$$

This result was obtained by using the classical density of states of the target corresponding to a fixed energy E and angular momentum L . Allowing L (or the eccentricity of the target orbit) to be randomly distributed, we obtain similar results for the probability and cross section averaged over L :

$$P_n(E, b) = P_1(n^2 E, b/n^2) \quad (14)$$

and

$$\sigma_n(E) = n^4 \sigma_1(n^2 E). \quad (15)$$

We now apply the classical scaling to the Klar-Wannier law

$$\sigma_1 = C(E - E_t)^\mu, \quad (16)$$

where $\mu = 2.65$ is Klar's exponent for the process with $e^- e^+ p$ in the final state [17]. For positron impact ionization of the H(1s) atom $E_t = 0.5$ a.u., and for the Ps(1s) breakup process $E_t = 0.25$ a.u. For an arbitrary n we obtain

$$\sigma_n = C n^{4+2\mu} (\Delta E)^\mu, \quad (17)$$

where

$$\Delta E = E - \frac{E_t}{n^2}. \quad (18)$$

It is important to note [32] that the classical scaling laws do not apply rigorously to quantal scattering because of the dimension of \hbar . In addition, in quantum theory the average over the angular momentum of the target is carried out by using the equation

$$\sigma_n = \frac{1}{n^2} \sum_l (2l+1) \sigma_{nl}, \quad (19)$$

where l is the orbital angular momentum quantum number of the target. It is obvious therefore that the classical approach is less accurate for small n when the number of possible values of l , which is equal to n , is low.

V. RESULTS AND DISCUSSION

A. Ps- p collisions

In Fig. 1 we present cross sections for Ps breakup in collisions with protons, reaction (1). The cross section σ_1 obeys the Klar-Wannier law, Eq. (16), for energy up to 10 eV above the threshold energy, $E_t = 6.8$ eV. Such a wide range of validity of the threshold law follows from Wannier's derivation [4] based on the smallness of the parameter (Gaussian units),

$$\beta = \frac{\Delta E a}{e^2}, \quad (20)$$

where a is the reaction-zone radius, which for the $e^+ e^- p$ system is of the order of the Bohr radius, and e is the elementary charge. Therefore, we should expect the threshold law to be valid for ΔE smaller than 1 a.u. = 27.2 eV. These considerations could also explain the relatively narrow range of validity

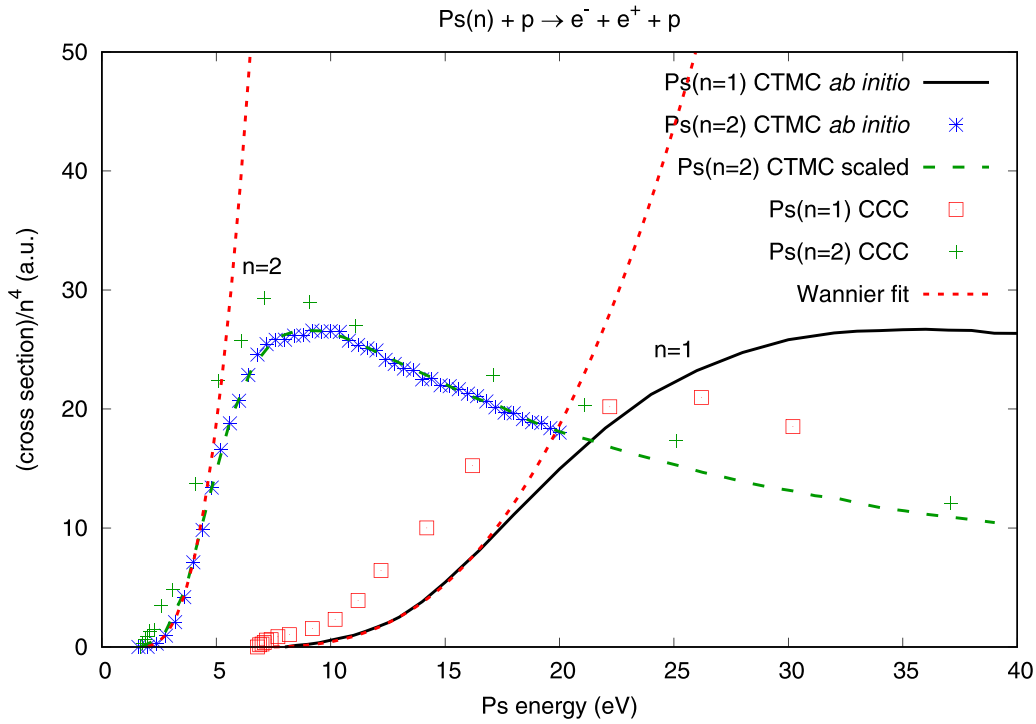


FIG. 1. Ps breakup in $Ps(n)+p$ collisions. The Klar-Wannier fit is shown by short-dashed lines. Dashed line: the $n = 2$ results obtained from scaling of the $n = 1$ data. Stars: CTMC results for $n = 2$. Both sets of data for $n = 2$ are divided by $2^4 = 16$.

of the Klar-Wannier law in the process of positron-impact ionization of Ar [24] since the reaction radius is much larger in this case compared to that for the process of ionization of hydrogen.

The quantum cross section for the $Ps(n = 1)$ breakup, although it qualitatively agrees with the CTMC result, is substantially higher near the threshold and peaks at a lower energy than the CTMC cross section. For the $Ps(n = 2)$ breakup

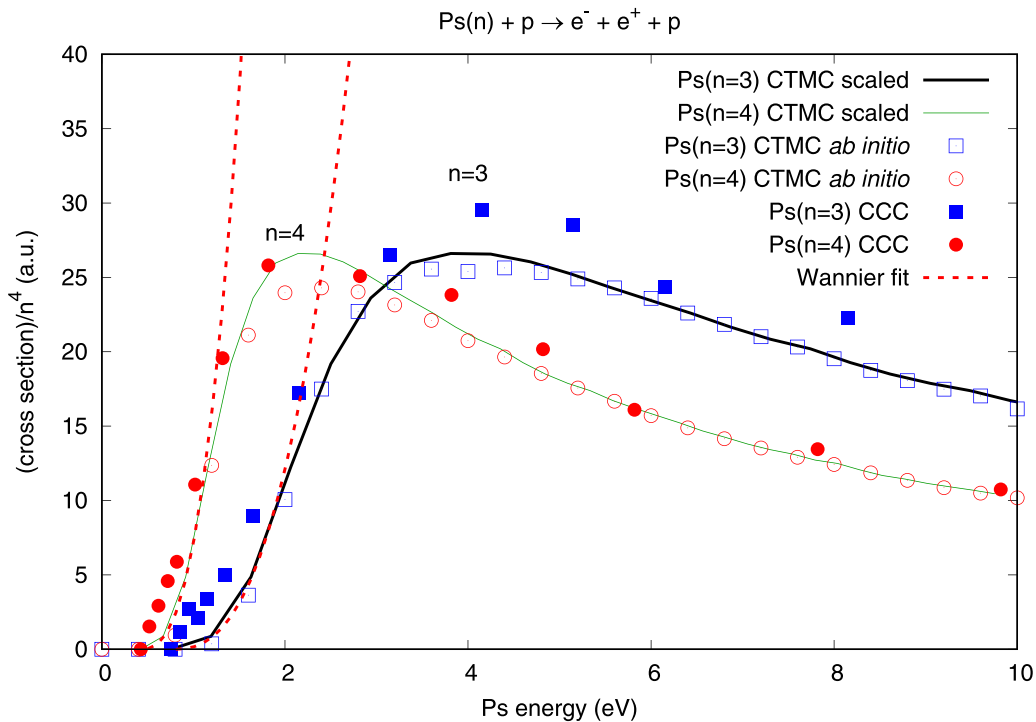


FIG. 2. Cross section for Ps breakup in $Ps(n)+p$ collisions for $n = 3$ and 4 , comparing the CTMC results with the CCC data.

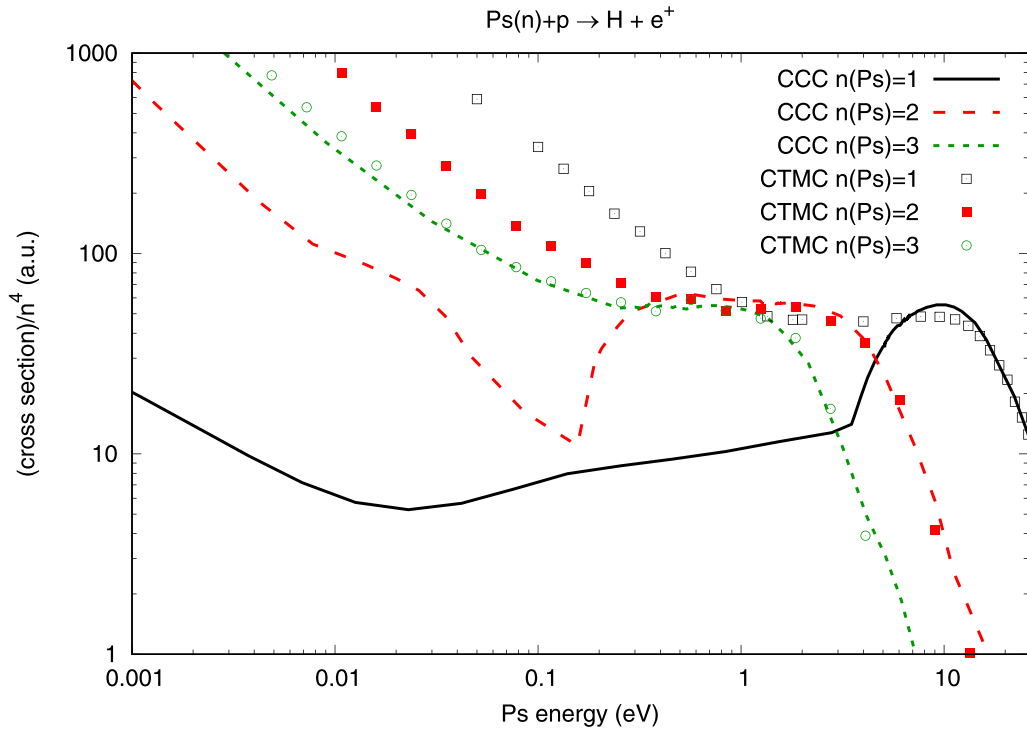


FIG. 3. H formation in $\text{Ps}+p$ collisions for $n(\text{Ps}) = 1, 2,$ and 3 , comparing CTMC and CCC [9] calculations.

the agreement is much better. We will address this issue in more detail in the next section on e^+ -H collisions.

The classical scaling, Eq. (9), describes very well the results of *ab initio* CTMC calculations. A similar picture is

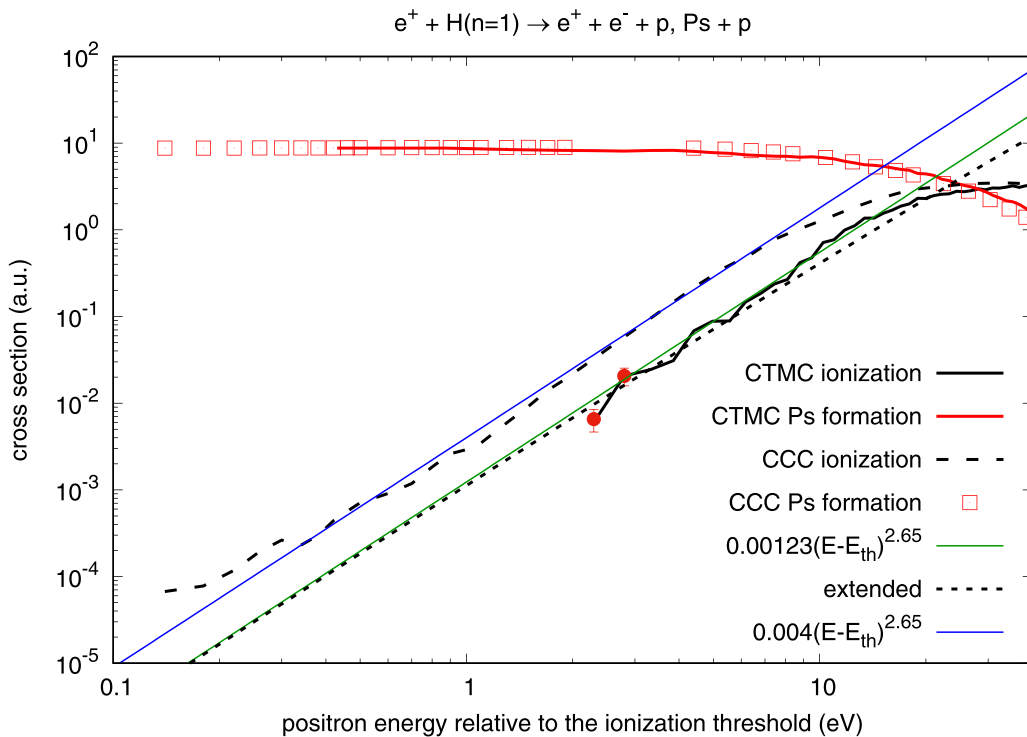


FIG. 4. Cross section for Ps formation and ionization in e^+ -H collisions. Solid lines: CTMC results and the Klar-Wannier fit to the ionization cross section; short-dashed line: the extension of the Klar-Wannier law [20]. The units for constants in the fit correspond to those used on the axes. Dashed line: CCC ionization [39]. Squares: CCC Ps formation. Solid circles with error bars indicate statistical uncertainty in the CTMC results for ionization.

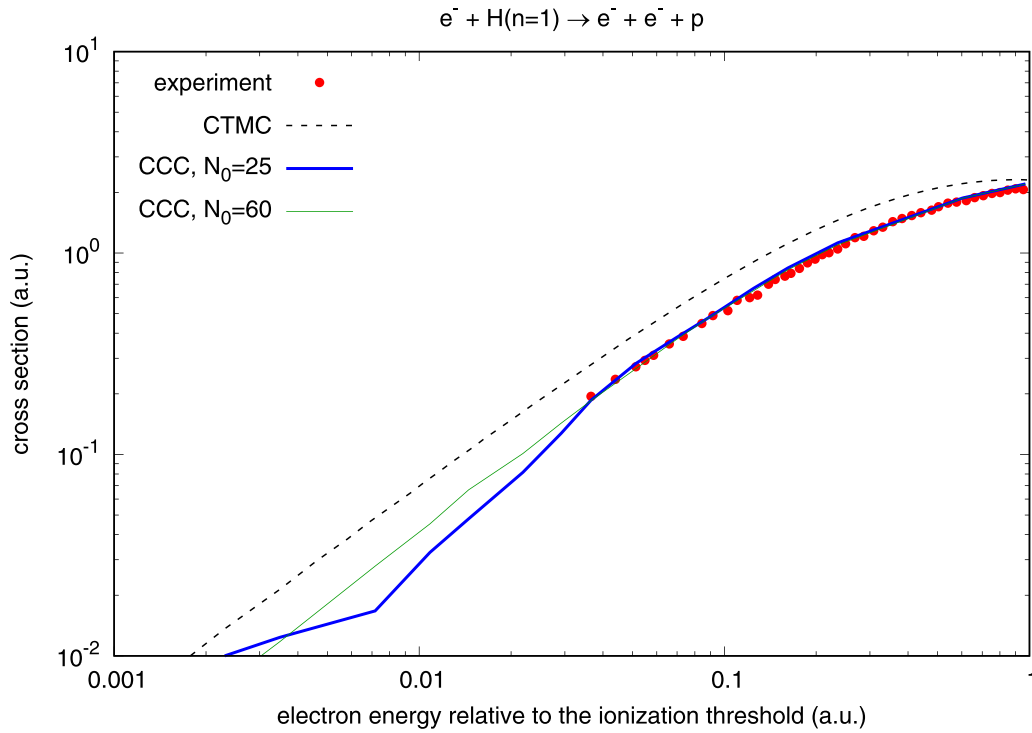


FIG. 5. Cross section for electron-impact ionization of H, comparing the CTMC results of Vranceanu [38] with CCC results employing the $N_0 = 25$ and $N_0 = 60$ bases (see text) and with experiment [40]. Note that the experimental error bars are too small to be visible on the scale of drawing.

observed in Fig. 2 for $n = 3$ and 4. The scaled results are somewhat different from the *ab initio* results reflecting statistical uncertainties of the CTMC calculations. The range of

the validity of the Klar-Wannier law squeezes according to the scaling law as $1/n^2$, being about 2.5, 1.0, and 0.65 eV above the threshold for $n = 2, 3$, and 4, respectively.

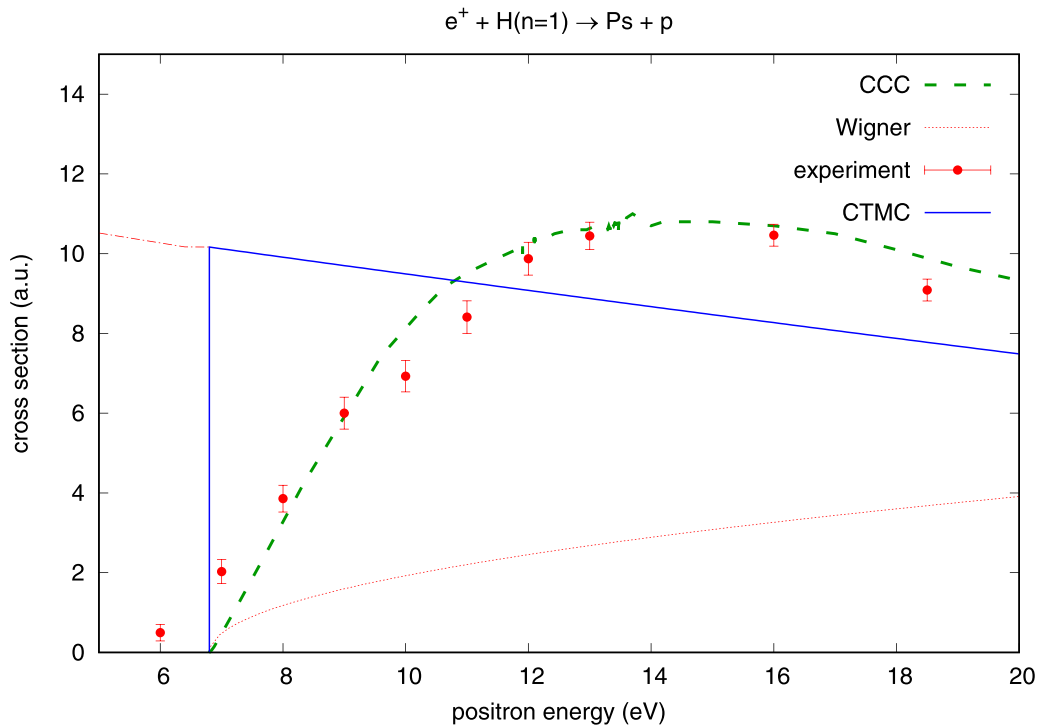


FIG. 6. Cross sections for Ps formation in $e^+H(1s)$ collisions, comparing CTMC, CCC [39], and experiment [43]. The dotted line is the Wigner law dependence with a proportionality constant of $1.08 \text{ a.u.}/(\text{eV})^{1/2}$. The dash-dotted red line is the unphysical CTMC cross section below the actual threshold (see text).

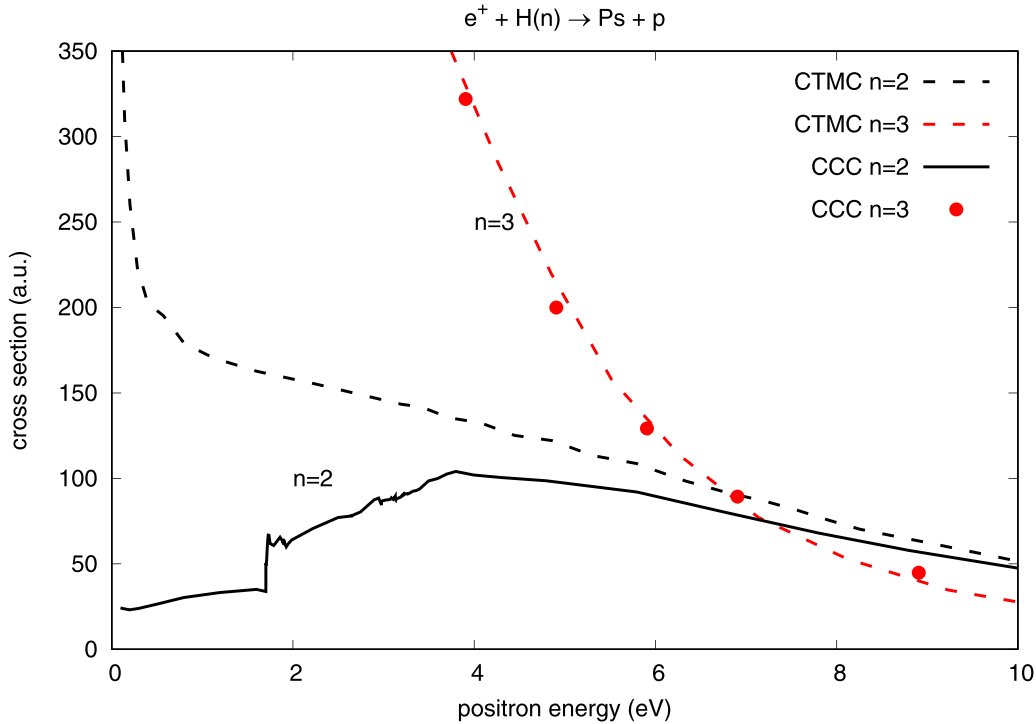


FIG. 7. $e^+ - H(n) \rightarrow \text{Ps} + p$ cross sections for $n = 2, 3$, comparing CTMC and CCC calculations.

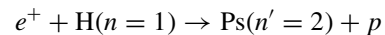
In Fig. 3 we present the cross section for the exothermic process of H formation in the same collision, reaction (2). Comparison with CCC results [9] shows strong disagreement at low energies for $n = 1$, where the classical cross section is very high and diverges as $1/E$, in contrast to the quantum result, which obeys the quantum Bethe-Wigner law for the exothermic reaction, Eq. (6), and whose absolute value is two orders of magnitude lower at E below 0.1 eV. It is apparent that the low-energy region in this case is a pure quantum domain since the Ps wavelength in this region is much longer than the range of Ps- p interaction. Note also that the scaled cross sections, $\tilde{\sigma} = \sigma/n^4$, exhibit different n dependence in the low-energy region: whereas $\tilde{\sigma}$ produced by CCC calculations grows with n , $\tilde{\sigma}$ produced by CTMC decreases with n . However, near the three-body breakup threshold classical and quantum cross sections start to agree, and this agreement continues for higher energies. This observation confirms that in the Wannier region the classical approach is valid for the charge-transfer process. This means that the three-body dynamics in this energy region is described very well by classical mechanics. With the increase of the principal quantum number agreement between classical and quantum results spreads down to low energies [11]. This is consistent with the generalized correspondence principle [32] as well as with the quantum threshold law for collisions involving the interaction of the charged particle with excited hydrogenlike systems, Eq. (7) [26,27]. Note that for $n = 2$, although both classical and quantum cross sections behave as C/E , the coefficient C is substantially different in the two theories, and the range of validity of this dependence is very different as well. However, already for $n = 3$ agreement is excellent. This reflects the fast growth of the Ps dipole moment with n .

B. $e^+ - \text{H}$ collisions

Another confirmation of the validity of classical mechanics near the three-body breakup threshold is the results for reactions (3) and (4) involving $e^+ + \text{H}$ collisions.

In Fig. 4 we present Ps formation and positron-impact ionization cross sections for positron collisions with the hydrogen atom in the ground state, reactions (3) and (4). The Wannier threshold law with Klar's exponent $\mu = 2.65$ is reproduced quite well, taking into account that the number of trajectories near the threshold should be enormous (about two orders of magnitude higher than in the region far from the threshold) due to the instability of the "Wannier-ridge" trajectories near the three-body breakup threshold [4]. However, the extension [20] of the Klar-Wannier law does not show improvement. To show the statistical uncertainty near the threshold, two points on the graph are shown with error bars, estimated by standard root-mean-square deviation, although the actual uncertainty can be larger. By varying the exponent μ while fitting the cross section to the Klar-Wannier law, we were able to estimate its uncertainty as $\Delta\mu = \pm 0.06$.

Near the three-body breakup threshold ($E_t = 13.6$ eV) the contribution of the excited Ps states to charge transfer, reaction (4), is very insignificant: the channel



contributes only 0.13 a.u., and higher n' contribute virtually nothing. Agreement with CCC calculations [39] is very good for the Ps formation process, but some differences can be seen when the cross sections are plotted on a linear scale (see Fig. 6 below). However, for the ionization process disagreement increases with decreasing energy. We note that in the near-threshold region ($\Delta E < 3$ eV) both classical and

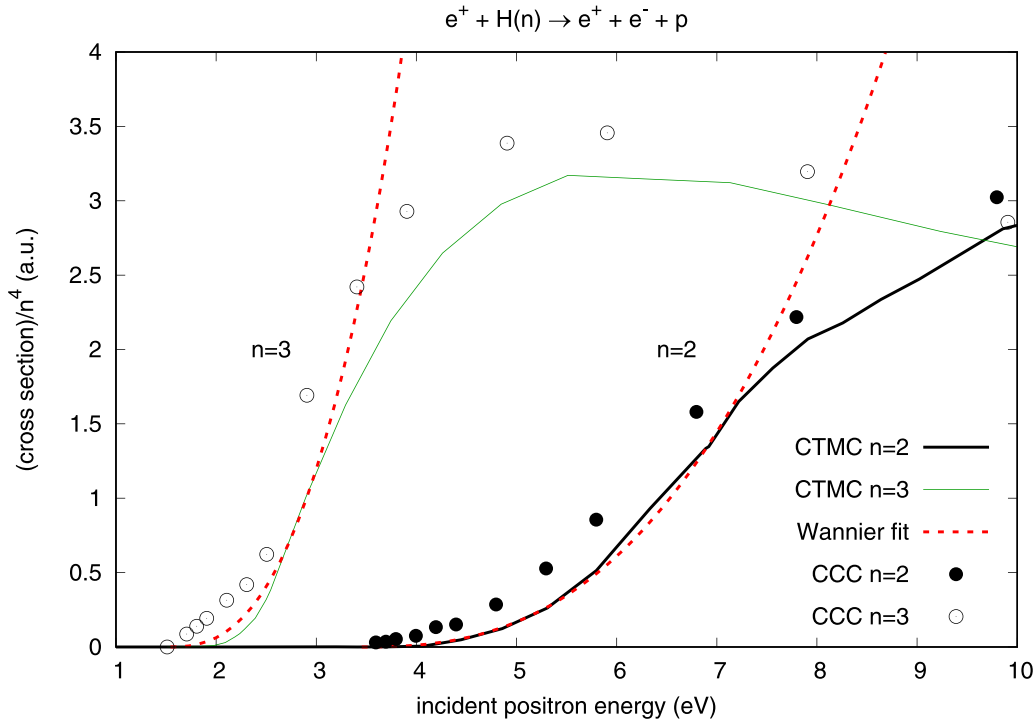


FIG. 8. $e^+H(n) \rightarrow p + e^+ + e^-$ cross sections for $n = 2, 3$, comparing CTMC and CCC calculations.

quantum methods suffer from substantial uncertainties. The CTMC method for breakup cross sections in this region requires a very large number of trajectories, and the CCC results are affected by poor convergence when the cross section becomes very small [39]. Still, it is observed that although both CTMC and CCC results obey the Klar-Wannier law, the CCC results for the ionization are systematically higher near the threshold, so that the coefficient C in the Klar-Wannier law, Eq. (16), obtained from the CCC calculations exceeds the CTMC result by a factor of 3.25. At this point it is unclear whether disagreement between CTMC and CCC is due to numerical uncertainties or due to some inherent defects in the classical theory. To shed more light on this issue, in Fig. 5 we present a comparison of the cross section for electron-impact ionization of H. CTMC results are taken from Vrinceanu [38] using the classical parameter $l/n = 0.1$, and the CCC results were obtained using Laguerre bases with $N_l = 25 - l$ and $N_l = 60 - l$, with $\lambda_l = 1$ for $l \leq l_{\max} = 6$. Both CCC calculations agree with experiment [40] where available. However, the larger CCC results converge to the Wannier law, with the Wannier exponent $\mu = 1.127$, better than the smaller ones, indicating the importance of large expansions when studying near-threshold breakup. The same energy dependence is observed for the CTMC results, but again, the absolute values are somewhat different, with the CTMC results exceeding those of CCC. We note that the classical microcanonical distribution cannot properly describe the probability density in s states, and this is the most likely reason for the difference [38]. However, we expect that with the growth of n , when states with more orbital angular momenta appear, the classical l -averaged cross section should approach the quantum-calculated one.

Overall, the comparison of CTMC with CCC results allows us to conclude that the three-body dynamics in this energy

region is described reasonably well by classical mechanics. Above the threshold our CTMC results also agree with the earlier calculations of Ohsaki *et al.* [14], and near the threshold they agree with the recent calculations of Liu *et al.* [16].

The CTMC calculations in [16] employ the so-called Heisenberg correction [41] to the Coulomb potential to incorporate the Heisenberg uncertainty principle in the treatment of the collisional process. The present results show that this procedure is unnecessary in the Wannier region, where the classical treatment works fine. The Heisenberg correction has been shown to stabilize bound states when they are calculated with classical mechanics [41]. For systems containing more than one electron the energy-bound correction was proposed [42] to prevent autoionization forbidden by quantum mechanics. However, at low collision energies, when one of the reactants is a neutral particle, the classical mechanics fails completely, and it is unlikely that its deficiency could be fixed with the Heisenberg potential or the energy-bound potential.

We continue the discussion of the Ps formation process (4) by extending the energy range below the three-body breakup threshold. In Fig. 6 we present the Ps formation results in the near-threshold region and compare them with CCC calculations [39] and experimental data [43]. The CTMC cross sections have been averaged over artificial oscillations, as discussed in the Appendix. The failure of the classical theory in this region is apparent: while the classical cross section is finite at the threshold, the quantum cross section starts from the zero value at the threshold, according to the Wigner law. This is a typical case of quantum suppression [3]. Moreover, classically, the process of Ps formation can occur below the actual threshold because the energy of the Ps($1s$) state is not bounded from below. This unphysical behavior is indicated in Fig. 6 by the dash-dotted red line, whereas the vertical

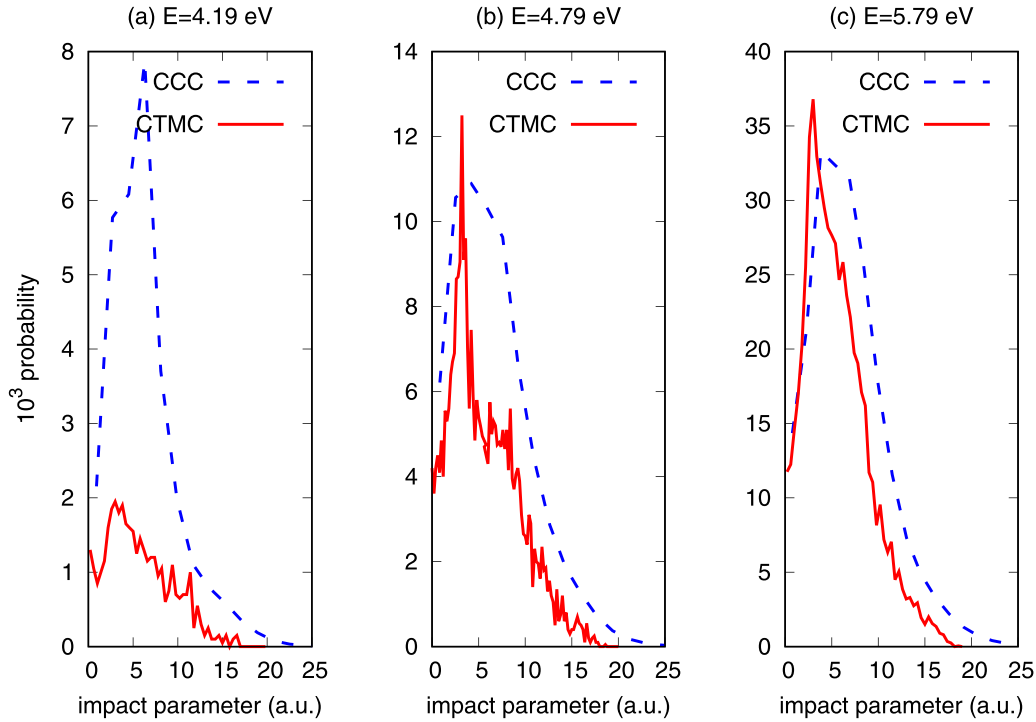


FIG. 9. $e^+H(n) \rightarrow p + e^+ + e^-$ probability as a function of the impact parameter for $n = 2$ and three selected energies, comparing CTMC and CCC calculations.

threshold onset at $E = 6.8$ eV is artificial from the classical point of view.

We have attempted to fit the CCC cross section near the threshold by the function $C(E - E_t)^{1/2}$, in accordance with the Wigner law, where C was chosen to reproduce the CCC cross section at $E - E_t = 0.2$ eV. It is apparent from Fig. 6 that the range of validity of the Wigner law is much narrower than that for the Klar-Wannier law. This can be understood from the basic physics of the ionization process versus the Ps formation process. In the first (classical) case the range of validity follows from $\beta \ll 1$ [4], where β is given by Eq. (20), which leads to $\Delta E \ll 1$ a.u. = 27.2 eV. In contrast, the quantum-mechanical Wigner law is based on the assumption that the wavelength of the outgoing particle is much greater than the reaction radius a , or $k < 1/a$. The reaction radius for Ps formation can be estimated as $a = 4$ a.u. Then we get $\Delta E < 1/(2ma^2) = 1/64$ a.u. = 0.42 eV, where $m = 2$ a.u. is the Ps mass.

In Fig. 7 we present cross sections for Ps formation in collisions of e^+ with excited hydrogen calculated using the CTMC and CCC methods. The CTMC data are in agreement with the classical scaling laws. The process is exothermic for both $n = 2$ and $n = 3$. For $n = 2$ disagreement between CTMC and CCC is very large in the low-energy region, although at $n = 3$ agreement is much better. Because of the nonzero dipole moment of the H atom in the excited state, the quantum cross section diverges as $1/E$ even for $n = 2$; however, its absolute value is very different from the classical one in this case. This is in sharp contrast to the three-body breakup behavior. Also, the $n = 2$ quantum cross section exhibits a stepwise structure at the threshold for Ps formation in the excited $n' = 2$ state. The onset is in accord with the Gailitis-Damburg threshold law [26], which predicts that reactions leading to the

formation of a charged fragment and a hydrogenlike fragment in an excited state have a finite cross section at the threshold. This structure is absent in the classical cross section since the energy levels in these calculations are not quantized.

In Fig. 8 we present the positron-impact ionization of H from the excited states, reaction (3). The CTMC results near the threshold can be fitted by the Klar-Wannier law, as shown in Fig. 8. The fit works for $n = 2$ for energies of about 3.5 eV above the threshold, whereas for $n = 3$ the range of validity of the Klar-Wannier law narrows down to about 1 eV above the threshold. As in the case of $n = 1$, the CCC cross sections are somewhat higher than the CTMC ones. More of a concern is that the CCC cross section cannot be fit by the Klar-Wannier law. A similar discrepancy was found in the Ps breakup cross sections in Ps- p/\bar{p} collisions [12]. To investigate the matter further we plot the classical probability for ionization of $H(n = 2)$ as a function of the impact parameter b and compare it with its quantum analog calculated from the CCC cross sections as

$$P_{\text{quant}} = \frac{\sigma^L k}{2\pi b},$$

where b is determined from the angular momentum as

$$b = \left(L + \frac{1}{2} \right) / k. \quad (21)$$

Since we use the classical relation between b and L , L in Eq. (21) should be understood as the angular momentum of the incident e^+ . On the other hand, in CCC calculations L is the total orbital angular momentum of the system, which creates some uncertainty in the CTMC-CCC comparison which decreases with increasing L . In Fig. 9 we present a probability comparison for three selected energies close to the ionization

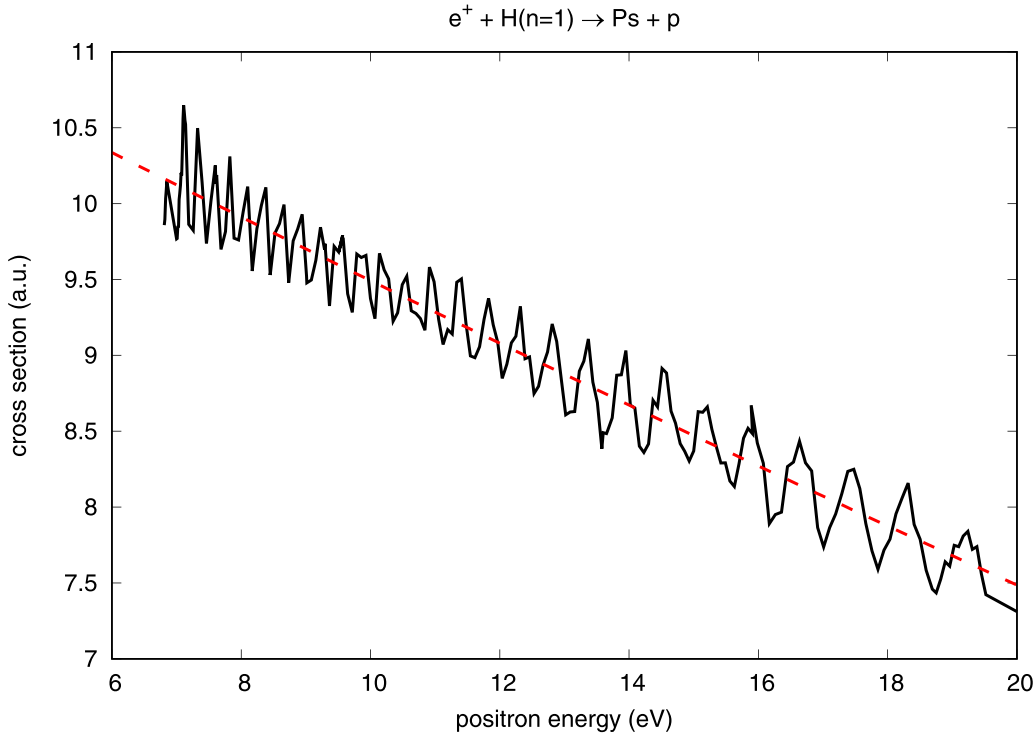


FIG. 10. Ps formation cross section in $e^+ - H(n=1)$ collisions in the energy range from the threshold to 20 eV. Solid line: CTMC calculations with a fixed initial positron position; dashed line: cross section averaged over oscillations.

threshold, $E_t = 3.40$ eV. For the lowest considered energy, $E = 4.19$ eV, the statistical uncertainty of the CTMC calculations is quite large, but it decreases from about 30% at $E = 4.19$ eV to about 5% at $E = 5.79$ eV, whereas the error caused by treating the collision angular momentum as a continuous quantity remains about 30% for all depicted curves. The latter error was estimated as being due to uncertainty in b , calculated as $\Delta b = 0.5/k$, and the actual error might be somewhat lower. Nevertheless, disagreement between CCC and CTMC calculations certainly exceeds both errors. Whereas for large impact parameters the disagreement can be explained by the neglect of tunneling in classical calculations, the reason for strong disagreement at the position of the peak is unclear. It is interesting that the effect is opposite quantum suppression found in cross sections for hydrogen formation in Ps- p collisions [31]. In that case quantum-mechanical probability is substantially lower than the classical one for low impact parameters, which results in the lower integrated cross section.

Farther away from the threshold the classical and quantum probabilities start to converge, except at larger impact parameters, where quantum $P(b)$ continues to be higher. However, the relative difference in integrated cross sections becomes small.

VI. CONCLUSION

While, in general, classical and quantum cross sections for reactions involving the three-body system e^+e^-p are convergent at a high principal quantum number n of the reactant (Ps or H), the near-threshold region is of special interest. In the present paper we have shown that near the three-body breakup threshold, the classical and quantum results for three-body breakup and charge transfer agree reasonably

well, even for $n = 1$, in terms of both energy dependence and absolute values, although some disagreement in the absolute value of the near-threshold positron-impact ionization cross section is observed. For scattering from the ground state disagreement is likely due to the inability of the classical microcanonical distribution to reproduce the quantum probability density. However, in general, the classical mechanics works reasonably well in the Wannier region. In contrast, the threshold behavior of the charge-transfer reaction in Ps- p and $e^+ - H$ collisions is very different in the classical and quantum theories. For $n = 1$ the classical results fail completely for both energy dependence and the absolute value. For $n = 2$, although classical and quantum functional behaviors for the exothermic charge transfer are similar, the quantitative disagreement is still very large. For higher n the classical and quantum versions converge quickly. Since classical calculations are computationally less expensive than quantum ones, these conclusions provide a useful guide for future calculations of reactions involving three particles interacting via Coulomb's law. The unresolved question is related to the near-threshold behavior of the CCC e^+ -impact ionization cross section from excited states. For $n > 1$ the present $N_0 = 25$ CCC calculations do not obey the Klar-Wannier law, similar to what was observed in Ps-breakup cross sections [12]. This problem requires further investigation but is most likely due to numerical limitations associated with having a too small Laguerre basis for the problem of interest.

ACKNOWLEDGMENTS

The Curtin authors acknowledge the Texas Advanced Computing Center (TACC) at The University of Texas

at Austin, the Australasian Leadership Computing Grants scheme of the National Computing Infrastructure, and The Pawsey Supercomputer Center for providing HPC resources and also the support of the Australian Research Council. H.B.A., J.S., and I.I.F. were supported by the U.S. National Science Foundation under Grant No. PHY-1803744 and by resources of the Holland Computing Center of the University of Nebraska, which receives support from the Nebraska Research Initiative.

APPENDIX: OSCILLATIONS IN CLASSICAL PS FORMATION CROSS SECTIONS

Cross sections for charge transfer plotted as a function of the projectile energy on a finer energy scale exhibit oscillations. For example, cross sections for Ps formation in e^+ -H collisions oscillate with a period which varies between 0.5 and 0.8 eV in the energy range between the threshold and 20 eV, as shown in Fig. 10. These oscillations are regular and cannot be attributed to statistical uncertainties. However, this is an artificial effect caused by a fixed starting point for the running trajectory. To show this, consider a positron incident on a H atom with a zero impact parameter and initial velocity v . Consider for simplicity a circular electron trajectory, and neglect the e^+ -H interaction. Then the electron trajectory is described by the equations

$$x_- = r \cos(\omega t - \phi), \quad y_- = r \sin(\omega t - \phi),$$

where r is the radius of the trajectory, ω is the angular frequency, and $-\phi$ is a random initial phase. The positron trajectory is described by the equations

$$x_+ = x_0 - vt, \quad y_+ = 0,$$

where x_0 is the positron's initial position. For effective charge transfer we require $\mathbf{r}_- = \mathbf{r}_+$. Then we obtain

$$\sin(\omega t - \phi) = 0, \quad t = (\pi + \pi k + \phi)/\omega,$$

where k is an integer. Solving now

$$r \cos(\omega t - \phi) = x_0 - vt,$$

we obtain

$$v_k = \frac{x_0 - r \cos(\omega t - \phi)}{t} = \frac{\omega[x_0 + (-1)^k r]}{\pi(k+1) + \phi}. \quad (\text{A1})$$

These values of velocity correspond to events that occur when the charge transfer is most likely. Although v_k depends on the random quantity ϕ , this dependence is weak since k should be large for moderate values of v_k . Indeed, for the ground state $\omega = 1$ a.u., and x_0 is typically several hundred atomic units; therefore, k should be of the order of 100. Averaging (A1) over ϕ , we obtain

$$\langle v_k \rangle = \frac{1}{2\pi} \int_0^{2\pi} v_k(\phi) d\phi = \omega \frac{[x_0 + (-1)^k r]}{2\pi} \ln \frac{k+3}{k+1}.$$

Using $r \ll x_0$ and $k \gg 1$, we obtain

$$v_k = \frac{x_0 \omega}{\pi k},$$

and the corresponding values of energy are

$$E_k = \frac{1}{2} \left(\frac{x_0 \omega}{\pi k} \right)^2.$$

The value of k corresponding to the peak at $E = E_k$ is

$$k = (2E_k)^{-1/2} \frac{x_0 \omega}{\pi},$$

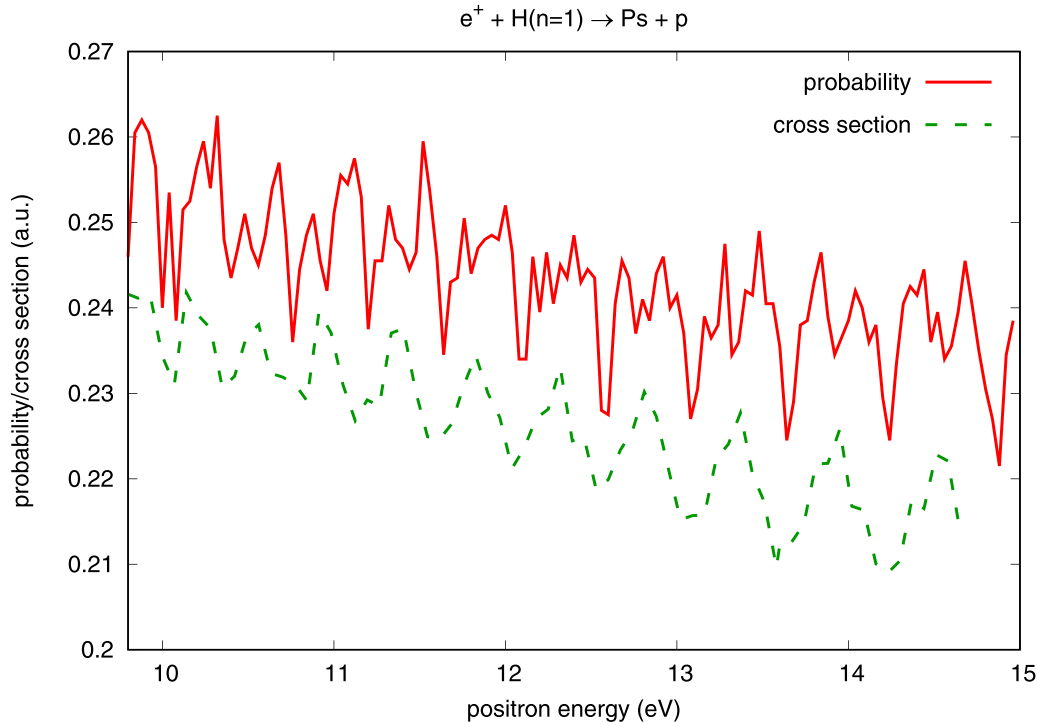


FIG. 11. Probability of Ps formation in e^+ -H($n = 1$) collisions for impact parameter $b = 2$ a.u. The lower curve is the cross section in atomic units divided by 40, which incorporates all impact parameters.

and the distance between peaks is

$$\Delta E_k = \frac{2E_k}{k}.$$

With the increase of E_k , the distance between peaks grows as $(2E)^{3/2}$, which is in agreement with the numerical results. Furthermore, for $x_0 = 300$ a.u., $E_k = 13.6$ eV; for example, we obtain $k = 95$ and $\Delta E_k = 0.28$ eV, compared to the computed $\Delta E_k = 0.5\text{--}0.6$ eV. Agreement is reasonable for such a simplistic estimate. The discussed effects can also be observed for the probability as a function of E for a fixed impact parameter b . In Fig. 11 we plot the probability for $b = 2$ a.u. and compare it with the cross section (divided by 40 for a better view). The probability exhibits some statistical uncertainties, but it is clear that its maxima match the maxima

in the cross section. Since a similar dependence is observed for other impact parameters, the oscillations do not disappear after integration over b .

For a given energy E the oscillation frequency grows with the growth of x_0 , and for $x_0 \rightarrow \infty$ it becomes indefinitely large, whereby the average over an arbitrarily small interval of energies gives the physical value of the probability and the cross section. In fact, there is no need to go to very large values of x_0 . Even for x_0 values of about 300 a.u. the average over the oscillation period gives accurate enough values of physical cross sections. We demonstrate this by presenting in Fig. 10 cross sections averaged over oscillations which give physically meaningful values. Since the average of oscillations over E is equivalent to the average over x_0 , the oscillations should not appear in quantum-mechanical calculations where the plane wave has an infinite uncertainty in x_0 .

-
- [1] H. R. Sadeghpour, J. L. Bohn, M. J. Cavagnero, B. D. Esry, I. I. Fabrikant, J. H. Macek, and A. R. P. Rau, *J. Phys. B: At. Mol. Opt. Phys.* **33**, R93 (2000).
- [2] E. P. Wigner, *Phys. Rev.* **73**, 1002 (1948).
- [3] R. Côté, E. J. Heller, and A. Dalgarno, *Phys. Rev. A* **53**, 234 (1996).
- [4] G. H. Wannier, *Phys. Rev.* **90**, 817 (1953).
- [5] R. Peterkop, *J. Phys. B: At. Mol. Phys.* **4**, 513 (1971).
- [6] A. R. P. Rau, *Phys. Rev. A* **4**, 207 (1971).
- [7] L. D. Landau and E. M. Lifshitz, *Quantum Mechanics (Nonrelativistic Theory)* (Pergamon, Oxford, 1977).
- [8] A. S. Kadyrov and I. Bray, *Phys. Rev. A* **66**, 012710 (2002).
- [9] A. S. Kadyrov, C. M. Rawlins, A. T. Stelbovics, I. Bray, and M. Charlton, *Phys. Rev. Lett.* **114**, 183201 (2015).
- [10] A. S. Kadyrov, I. Bray, M. Charlton, and I. I. Fabrikant, *Nat. Commun.* **8**, 1544 (2017).
- [11] M. Charlton, H. B. Ambalampitiya, I. I. Fabrikant, D. V. Fursa, A. S. Kadyrov, and I. Bray, *Phys. Rev. A* **104**, L060803 (2021).
- [12] M. Charlton, H. B. Ambalampitiya, I. I. Fabrikant, I. Kalinkin, D. V. Fursa, A. S. Kadyrov, and I. Bray, *Phys. Rev. A* **107**, 012814 (2023).
- [13] R. Abrines and I. C. Percival, *Proc. Phys. Soc.* **88**, 861 (1966).
- [14] A. Ohsaki, T. Watanabe, K. Nakanishi, and K. Iguchi, *Phys. Rev. A* **32**, 2640 (1985).
- [15] A. E. Wetmore and R. E. Olson, *Phys. Rev. A* **34**, 2822 (1986).
- [16] S. Liu, D. Ye, and J. Liu, *Phys. Rev. A* **101**, 052704 (2020).
- [17] H. Klar, *J. Phys. B: At. Mol. Phys.* **14**, 4165 (1981).
- [18] J. M. Rost and E. J. Heller, *Phys. Rev. A* **49**, R4289(R) (1994).
- [19] W. Ihra, J. H. Macek, F. Mota-Furtado, and P. F. O'Mahony, *Phys. Rev. Lett.* **78**, 4027 (1997).
- [20] K. Jansen, S. J. Ward, J. Shertzer, and J. H. Macek, *Phys. Rev. A* **79**, 022704 (2009).
- [21] A. S. Kadyrov, I. Bray, and A. T. Stelbovics, *Phys. Rev. Lett.* **98**, 263202 (2007).
- [22] G. O. Jones, M. Charlton, J. Slevint, G. Laricchia, A. Kövér, and M. R. Poulsen, and S. N. Chormaic, *J. Phys. B: At. Mol. Opt. Phys.* **26**, L483 (1993).
- [23] P. Ashley, J. Moxom, and G. Laricchia, *Phys. Rev. Lett.* **77**, 1250 (1996).
- [24] T. J. Babij, J. R. Machacek, D. J. Murtagh, S. J. Buckman, and J. P. Sullivan, *Phys. Rev. Lett.* **120**, 113401 (2018).
- [25] H. A. Bethe, *Phys. Rev.* **47**, 747 (1935).
- [26] M. Gailitis and R. Damburg, *Proc. Phys. Soc.* **82**, 192 (1963).
- [27] M. Gailitis, *J. Phys. B: At. Mol. Phys.* **15**, 3423 (1982).
- [28] I. I. Fabrikant, A. W. Bray, A. S. Kadyrov, and I. Bray, *Phys. Rev. A* **94**, 012701 (2016).
- [29] D. Krasnicky, R. Caravita, C. Canali, and G. Testera, *Phys. Rev. A* **94**, 022714 (2016).
- [30] D. Krasnicky, G. Testera, and N. Zurlo, *J. Phys. B: At. Mol. Opt. Phys.* **52**, 115202 (2019).
- [31] H. B. Ambalampitiya, D. V. Fursa, A. S. Kadyrov, I. Bray, and I. I. Fabrikant, *J. Phys. B: At. Mol. Opt. Phys.* **53**, 155201 (2020).
- [32] R. Abrines and I. C. Percival, *Proc. Phys. Soc.* **88**, 873 (1966).
- [33] I. C. Percival and D. Richards, *Adv. At. Mol. Phys.* **11**, 1 (1976).
- [34] H. B. Ambalampitiya, J. Stallbaumer, and I. I. Fabrikant, *Phys. Rev. A* **105**, 043111 (2022).
- [35] S. J. Aarseth and K. Zare, *Celestial Mechanics* **10**, 185 (1974).
- [36] H. B. Ambalampitiya, Ph.D. thesis, University of Nebraska-Lincoln, 2021.
- [37] L. D. Landau and E. M. Lifshitz, *Mechanics*, 3 ed. (Pergamon, Oxford, 1969).
- [38] D. Vrinceanu, *Phys. Rev. A* **72**, 022722 (2005).
- [39] I. Bray, A. W. Bray, D. V. Fursa, and A. S. Kadyrov, *Phys. Rev. Lett.* **121**, 203401 (2018).
- [40] M. B. Shah, D. S. Elliott, and H. B. Gilbody, *J. Phys. B: At. Mol. Phys.* **20**, 3501 (1987).
- [41] C. L. Kirschbaum and L. Wilets, *Phys. Rev. A* **21**, 834 (1980).
- [42] J. S. Cohen, *Phys. Rev. A* **54**, 573 (1996).
- [43] S. Zhou, H. Li, W. E. Kauppila, C. K. Kwan, and T. S. Stein, *Phys. Rev. A* **55**, 361 (1997).